



**3D RECONSTRUCTION OF MAMMOGRAM USING  
RADON TRANSFORM WITH TWO VIEWS**



**A PROJECT REPORT**

*Submitted by*

**NANCY PRIYA S**

**Reg. No: 15MAE008**

*In partial fulfillment for the requirement of award of the degree*

*of*

**MASTER OF ENGINEERING**

*in*

**APPLIED ELECTRONICS**

**Department of Electronics and Communication Engineering**

**KUMARAGURU COLLEGE OF TECHNOLOGY**  
(An autonomous institution affiliated to Anna University, Chennai)

**COIMBATORE - 641 049**

**ANNA UNIVERSITY: CHENNAI 600 025**

**APRIL-2017**



## **BONAFIDE CERTIFICATE**

Certified that this project report titled “**3D RECONSTRUCTION OF MAMMOGRAM IMAGES USING RADON TRANSFORM WITH TWO VIEWS** ” is the bonafide work of **NANCY PRIYA S [Reg. No. 15MAE008]** who carried out the research under my supervision. Certified further that, to the best of my knowledge the work reported here in does not form part of any other project or dissertation on the basis of which a degree or award was conferred on an earlier occasion on this or any other candidate.

**SIGNATURE**

**Ms. S.SASIKALA**

**PROJECT SUPERVISOR**

Department of ECE

Kumaraguru College of Technology

Coimbatore-641 049

**SIGNATURE**

**Prof. K. RAM PRAKASH**

**HEAD OF THE DEPARTMENT**

Department of ECE

Kumaraguru College of Technology

Coimbatore-641 049

The candidate with university **Register No.15MAE008** is examined by us in the project viva-voce examination held on.....

**INTERNAL EXAMINER**

**EXTERNAL EXAMINER**

## ACKNOWLEDGEMENT

First I would like to express my praise and gratitude to the Lord, who has showered his grace and blessing enabling us to complete this project in an excellent manner. He has made all things in beautiful in his time.

I express my sincere thanks to my beloved Joint Correspondent, **Shri. Shankar Vanavarayar** for his kind support and for providing necessary facilities to carry out the project work.

I would like to express my sincere thanks to our beloved Principal **Dr.R.S.Kumar M.E., Ph.D.**, who encouraged me with his valuable thoughts.

I would like to express my sincere thanks and deep sense of gratitude to my HOD, **Dr.K.Malarvizhi M.E.,Ph.D.**, and **Prof K. RamPrakash M.E.**, for their valuable suggestions and encouragement which paved way for the successful completion of the project.

I greatly privileged to express my deep sense of gratitude to the Project Coordinator and Supervisor **Ms. S. Sasikala M.Tech., (Ph.D)**, Associate Professor, for her continuous support throughout the course. In particular, I wish to thank and express my everlasting gratitude to her for the expert counselling in each and every steps of project work and I wish to convey my deep sense of gratitude to all teaching and non-teaching staff members of ECE Department for their help and cooperation.

Also I am very much thankful to the courtesy of TM Deserni, Dept. of Medical Informatics and RWTH Achen, Germany for providing their data to this research work.

Finally, I thank my parents and my family members for giving me the moral support in all of my activities and my dear friends who helped me to endure my difficult times with their unfailing support and warm wishes.

## **ABSTRACT**

The 3D reconstruction of mammogram images is the process of combining the pre-processed mammogram images into a 3D image for the purpose of finding the exact location of the abnormal growth in the breast. This is achieved by Radon transform. The pre-processing of mammogram images is an important aspect in the reconstruction of mammogram images in the field of mammography. Here the mammogram images obtained from CC (Cranio caudal view) and MLO (medio lateral view) are pre-processed in order to obtain information about the mammogram images. Hence the mammogram images deals with three steps in the pre-processing stage. In the first step, mammogram images are made noise free by adaptive median filter. In the second step, the de-noised mammogram images are enhanced using CLAHE (Contrast Limited Adaptive Histogram Equalization). In the third step, the pectoral muscle identification and segmentation is done by using Adaptive K means segmentation. The depth map is then estimated using stereo matching algorithm for matching CC and MLO views and then the 3-D reconstruction has been achieved by using Radon transform.

## TABLE OF CONTENTS

CHAPTER NO	TITLE	PAGE NO
	<b>ABTRACT</b>	iv
	<b>LIST OF FIGURES</b>	vii
	<b>LIST OF ABBREVIATIONS</b>	viii
1	<b>INTRODUCTION</b>	1
	1.1 BREAST CANCER	1
	1.2 BREAST CANCER STATISTICS	2
	1.3 MAMMOGRAPHY	2
	1.4 MAMMOGRAM PRE-PROCESSING	4
	1.5 MAMMOGRAM RECONSTRUCTION	5
	1.6 SOFTWARE USED	6
2	<b>LITERATURE SURVEY</b>	7
	2.1 NOISE REDUCTION	7
	2.2 IMAGE ENHANCEMENT	10
	2.3 IMAGE SEGMENTATION	12
	2.4. MATCHING CC AND MLO MAMMOGRAM	14
	2.5. 3D RECONSTRUCTION	15
3	<b>IMAGE DATABASE</b>	19
	3.1 DDSM	19
	3.2 INBREAST DATABASE	19
4	<b>PROPOSED WORK</b>	21
	4.1 PROPOSED WORK DIAGRAM FOR PHASE 1	21

	4.2 NOISE REDUCTION	22
	4.3 IMAGE ENHANCEMENT	22
	4.4 IMAGE SEGMENTATION	23
	4.5 DEPTH MAP ESTIMATION	26
	4.6. 3D RECONSTRUCTION OF TUMOR FROM MAMMOGRAM	30
	4.7 PERFORMANCE MEASURES	31
5	<b>RESULTS AND SIMULATION</b>	33
	5.1 NOISE REMOVAL USING ADAPTIVE MEDIAN FILTER	33
	5.2 IMAGE ENHANCEMENT - CC MAMMOGRAM	35
	5.3 IMAGE SEGMENTATION	37
	5.4 CLUSTERED CC -TUMOUR USING MEAN SHIFT ALGORITHM	39
	5.5 DEPTH MAP OF CC AND MLO VIEW MATCHED IMAGE	40
	5.6 RECONSTRUCTION USING 4 PROJECTIONS	41
	5.7 RECONSTRUCTION USING 180 PROJECTIONS	42
	5.8 SURFACE PLOT ODF 3D RECONSTRUCTED TUMOUR	43
	5.9 PERFORMANCE MESURES	44
6	<b>CONCLUSION AND FUTURE WORKS</b>	46
	<b>REFERENCES</b>	47
	<b>LIST OF PUBLICATION</b>	51

## LIST OF FIGURES

<b>FIG NO</b>	<b>TITLE</b>	<b>PAGE NO</b>
1.5	Breast Cancer Statistics	6
4.1	Proposed Work Diagram	20
4.2	Depth map estimation block diagram	26
5.1.1	Original And Denoised Mammogram	32
5.1.2	Original And Denoised Mammogram	33
5.1.3	Enhanced Mammogram Using CLAHE	34
5.1.4	Enhanced Mammogram Using CLAHE	35
5.1.5	Clustered Mammogram And Segmented Tumour From Mammogram	36
5.1.6	Clustered Mammogram And Segmented Tumour From Mammogram	37
5.1.7	Clustered Tumour Using Mean Shift Algorithm	38
5.1.8	Depth map of cc and mlo view matched image	39
5.1.9	Reconstruction Using 4 Projections	40
5.1.10	Reconstruction Using 180 Projections	41
5.1.11	Surface Plot of 3D Reconstructed Tumour	42

## LIST OF ABBREVIATIONS

ABBREVIATION	NOMENCLATURE
CC	Cranio Caudal
MLO	Medio Lateral Oblique
CLAHE	Contrast Limited Adaptive Histogram Equalization
HE	Histogram Equalization
DDSM	Digital Database for Screening Mammography
BI-RADS	Breast Imaging-Reporting and Data System
PSNR	Peak Signal To Noise Ratio
MSE	Mean-Squared Error
SSIM	Structured Similarity Index Measure
SIFT	Scale Invariant Feature Transform
ICP	Iterative Closest Point
SAD	Sum of Absolute Difference
GRAD	Gradient of Absolute Difference

# CHAPTER I

## INTRODUCTION

The goal of this project is the diagnosis of the breast malignancy in the early stage. The incorporation of data from two perspectives of the breast may enhance the execution of analysis. Pre-processing is the initial step of a conventional image processing pipeline. On account of mammograms, average pre-processing methods includes noise reduction, image enhancement, background exclusion, pectoral muscle identification and removal of pectoral muscle in order to avoid false positive. The 3D reconstruction of tumor from mammograms is used for locating the cancerous growth in the breast.

### 1.1 BREAST CANCER

Breast tumor is a sort of growth that creates from breast cells[1]-[5]. Breast tumor more often will not begin off in the inner layer of ducts or the lobules that supply them with drain. A dangerous tumor can spread to different parts of the body. A breast growth that begins off in the lobules is known as lobular carcinoma, while one that created from the ducts is called ductal carcinoma. On normal tissue, the cells are in continuous growth and division. If an abnormality arises, such as a mutation, the cell has a mechanism called apoptosis to program its own death.

A normal cell becomes a tumor cell, when a mutation occurs and it loses the ability to control its division rate. When that happens, the tumor cells grow and divide without being stimulated by growth factors. Moreover, they become insensitive to growth inhibitory signals and develop mutations that block apoptosis. In fact, most of the times, a tumor cell does not turn into a cancer. This happens when the mechanism of apoptosis does not work. As cancerous cells divide, they acquire high resistance and develop characteristics to assure their own survival. They develop the ability to induce the growth of new vessels (angiogenesis) to supply the essential nutrients for their rapid growth. They also develop other malignant characteristics, such as the ability to occupy the immune system, to mutate, to invade and metastabilize.

## 1.2 BREAST CANCER STATISTICS

Breast malignancy is the most widely recognized obtrusive disease in females around the world. It concerns 16% of every single female disease and 22.9% of intrusive tumors in female. 18.2% of all tumors around the world are from breast disease. Breast disease rates are much higher in developed countries compared with developing ones. The diverse ways of life and dietary patterns of females in rich and poor nations are likewise contributory components.

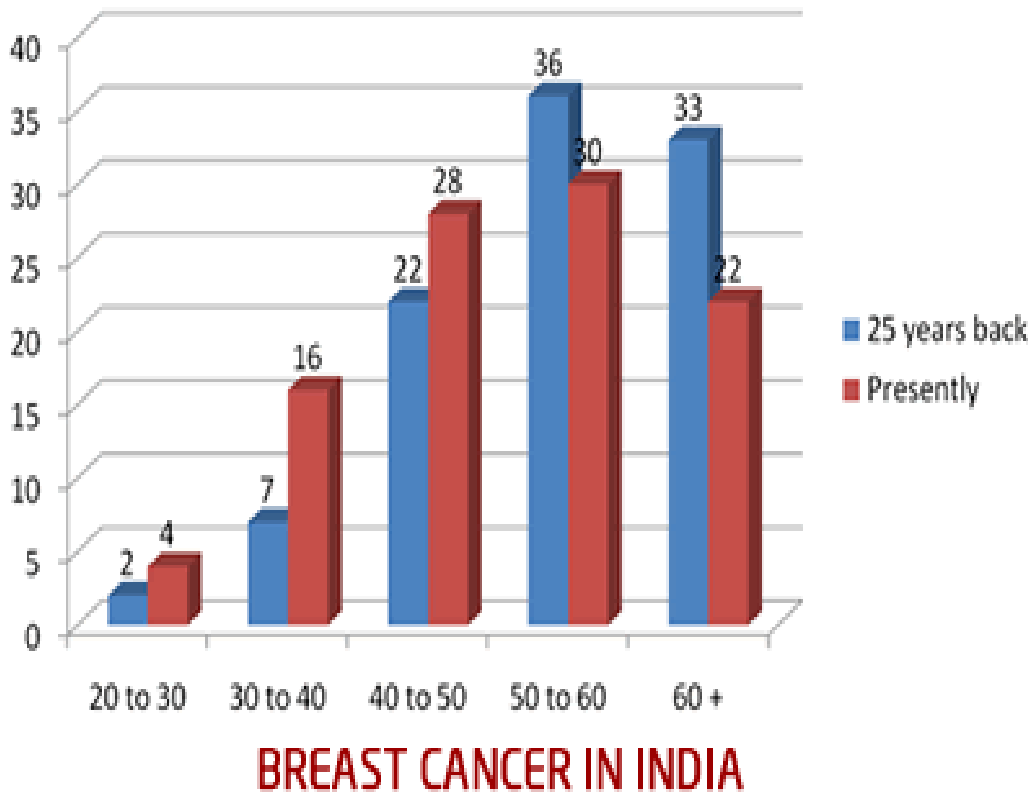


**Fig.1.1 Breast Cancer Statistics in India**

In Fig.1, the x axis represents the age and the y axis represents the percentage of the affected people.

## 1.3 MAMMOGRAPHY

Mammography is a specific type of breast imaging that uses low-dose X-rays to detect cancer early i.e., before women experience symptoms when it is most treatable [1]. It plays a

major role in early detection of breast cancers because it can show changes in the breast up to two years before a patient or physician can feel them. It can be used in the event when any irregularity or other indication of breast disease is found. A mammogram is an X-ray image of the breast. It is estimated that approximately 85% of breast cancers may be detected by mammography, though the sensitivities can vary according to the radiologist experience. Screening mammograms simply look for signs of cancer. These procedures are X-ray exams of the breasts done yearly in women who have no breast symptoms or changes in their breast exam. Two types of mammograms are taken into consideration.

1. Screening mammogram
2. Diagnostic mammogram

### **1.3.1 Screening mammogram**

The goal of a screening mammogram is to detect breast cancer as early as possible. In a screening mammogram, each breast is X-rayed in two different positions: from top to bottom and from side to side. When a mammogram image is viewed, breast tissue appears white and opaque and fatty tissue appears darker and translucent. The screening mammogram is extremely important in woman's health and as the age is a risk factor, women after age 40 should get mammograms once in every two years and yearly once after 50.

### **1.3.2 Diagnostic mammogram**

The diagnostic mammography differs little from screening mammography. It may involve more views and it is done when there is something suspicious. In addition, it can focus a specific area of the breast where the abnormality was detected. Mammograms can likewise be utilized to look at a patient's breast if she has a breast issue or a change is seen on a screening mammogram. When utilized in this way, they are called diagnostic mammograms. They may incorporate additional perspectives (views) of the breast that aren't some portion of screening mammograms.

Both screening and diagnostic mammography are traditionally performed by radiologists who visually inspect mammograms. One of the difficulties with mammography is that images

generally have low contrast. Mammograms show normal structures such as fat, fibro glandular tissue, breast ducts and nipples, as well as possible abnormalities. Although fat appears as black regions on mammograms, everything else appear as levels of white, making it hard to distinguish between normal and abnormal tissue. Manual screening is a tiring and tedious task prone to human error.

## **1.4 MAMMOGRAM PRE-PROCESSING**

Pre-processing an image is a fundamental task for correcting defects produced during the acquisition process of real time and its reproduction on its display, due to physical and technological limitations [7]. It can also be useful as a pre-processing stage in order to improve the results of higher level applications. The problem of removing the noise of an image while preserving its main features like edges, textures, colors, contrast, etc., has been extensively investigated over the last two decades and several types of approaches have been developed.

### **1.4.1 De-noising mammogram**

The noise present in the digital mammogram images directly points the competency of a classification problem [7]. Study reveals that the overall accuracy of classification systems decreases abruptly with increase in noise. The decrease can become as significant as 21%. This noise can be added due to several factors such as data acquisition and image preprocessing stage. Therefore, the main purpose of de-noising is to remove noise factors such as low contrast resolution, film noise, artifacts, etc., while preserving the desired signal as much as possible. De noising is often done before the images are to be analyzed. Consequently, de-noising plays a very important role in image segmentation, feature extraction and in the classification task.

### **1.4.2 Image enhancement**

The principle objective of Image enhancement is to process an image so that result is more suitable than original image for specific application [8]. Digital image enhancement techniques provide a multiple choices for improving the visual quality of images. Image enhancement is basically improving the interpretability or perception of information in images for human viewers and providing better input for other automated image processing techniques. The principal objective of image enhancement is to modify attributes of an image to make it

more suitable for a given task and a specific observer. During this process, one or more attributes of the image are modified. The choice of attributes and the way they are modified are specific to a given task. Moreover, observer-specific factors, such as the human visual system and the observer's experience, will introduce a great deal of subjectivity into the choice of image enhancement methods.

### **1.3.3 Segmentation**

The mammogram segmentation process is designed to find suspicious areas, and to separate the suspicious areas from the background that will be used for extracting features of suspicious regions[10]. Many thresholding techniques have been developed for image segmentation. In properly imaged MLO mammograms, the pectoral muscle is visible as a triangular region of high-density at the upper posterior part of the image. Its presence in mammograms poses an additional source of complexity in automated analysis as it may interfere with the results of image processing methods and induce a bias in breast cancer detection. The texture of the pectoral muscle may also be similar to some abnormalities and may cause false positives in the detection of suspicious masses. Exclusion of the pectoral muscle facilitates automatic breast tissue identification and allows the radiologist to check for the development of cancers in the area overlying the pectoral muscle.

Generally, the mammogram images are with unwanted noise, poor picture contrast, in homogeneity, feeble limits and disconnected parts which will influence the substance of the medical images. This issue corrected by preprocessing. The preprocessing is the key strides in the restorative image processing to create better picture quality for differentiation and highlight extractions. The pre-processing steps manage image improvement, noise and exceptional mark removal. The image segmentation can be used for removal of pectoral muscle.

## **1.5 MAMMOGRAM RECONSTRUCTION**

The mammogram images are obtained generally out of several views in order to combine it for reconstruction to find the exact location of the tumor[35]. But several views may lead to overdosage of radiation. Hence two views CC and MLO only are used. CC view is a top-down X-ray penetration on the breast almost covering the entire breast. MLO view is an X-ray

projection from shoulder to opposite hip diagonally. Mammograms taken by two perspectives: cranio-caudal (CC) and medio lateral oblique (MLO) views give just 2D projections of the abnormal growth, which do not have the profundity data. In this way, imagining the relative sore area from mammograms is a difficult task for radiologists. To help radiologists in finding and rendering sore tissues, reconstruction of mammogram cross sectioned data is needed.

## **1.6 SOFTWARE USED**

MATLAB R2014b

## CHAPTER 2

### LITERATURE SURVEY

This survey deals about the pre-processing of mammogram images, segmentation of tumor from the mammogram, pectoral muscle removal and 3D reconstruction of tumor from mammogram. Pre-processing is very important to change and adjust the mammogram image for further study and processing. This may include noise reduction, image enhancement. The second step is the segmentation of tumor from the mammogram and pectoral muscle removal. The segmentation of tumor from the mammogram is done for the segmenting the mammogram into different clusters and extracting the tumor part alone. The pectoral muscle removal is done to avoid false positive. The pectoral muscle appears as the level of white pixel since it is a dense muscle. The 3D reconstruction of tumor from mammogram is done for finding the exact location of the tumor concentration.

#### 2.1 NOISE REDUCTION

DDSM database images are used for the experimental study. There are different types of noise present in mammogram. Some of them are,

Quantum noise are dominant in mammogram. Noise level present in the images highly affect the quality and accuracy of classification when working with Mammographic images. Quantum noise occurs inherently in low dose X ray imaging due to the very low X – ray quantum counts.

Salt and pepper noise is also called impulse valued noise. Other terms are spike noise, random noise or independent noise. Due to this noise black and white dots appear in the image. The main reason behind the appearance of salt and pepper noise are sharp and sudden changes of image signal and dust particles in the image acquisition source or over heated faulty components [46]. Due to this noise, image is corrupted to a small extent.

Speckle noise can be considered as a multiplicative noise. This noise can exist in an image similar to Gaussian noise.

Poisson noise is also called photon noise. This noise is due to the statistical behavior of electromagnetic waves such as x-rays, visible lights and gamma rays. In a mammogram image poisson noise is due to the change in the number of photons in the mammogram unit. The root mean square value of this noise is proportional to the square root intensity of the image. Due to this noise, different pixel of the image are suffered by independent noise value.

### **2.1.1 Filtering**

#### **Max and Min filter**

The max and min filter is the order-statistics filter most used in image processing [1]-[5]. The maximum and minimum filters are shift-invariant. Whereas the minimum filter replaces the central pixel with the darkest one in the running window, the maximum filter replaces it with the lightest one.

#### **Mid-Point Filter**

The midpoint filter simply computes the midpoint between the maximum and minimum values in the area encompassed by the filter [6]. This filter combines order statistics and averaging. This filter works best for random distributed noise like Gaussian or uniform noise. The Midpoint filter blurs the image by replacing each pixel with the average of the highest pixel and the lowest pixel (with respect to intensity) within the specified window size.

### **2.1.2 Salt-Pepper Impulse Noise Detection And Removal Using Multiple Threshold.**

Another impulse technique to construct the choice govern and practice the limit work. The new impulse detection approach in light of various thresholds considers different neighborhood data of the channel window to judge whether impulse noise exists [3]. The new impulse finder is exceptionally exact avoiding an increase in computational complexity. The impulse detection algorithm is utilized before the separating procedure begins, and along these lines just the commotion tainted pixels are supplanted with the evaluated focal clamor free requested mean esteem in the present channel window. Broad exploratory results show that the new channel is fit for saving more points of interest while adequately stifling impulse commotion in undermined pictures. Impulse noise can appear because of a random bit error on a communication channel. In this work, the source images are corrupted only by salt-pepper

impulse noise, which means a noisy pixel has a high value due to positive impulse noise, or has a low value due to a negative impulse noise.

### **2.1.3 Wavelet Thresholding De-Noising**

Wavelet thresholding de-noising depends on the possibility that the vitality of the image to be characterized focuses on some wavelet coefficients, while the vitality of commotion spreads all through all wavelet coefficients [4]. Wavelet edge de-noising is an extremely productive technique, the reason for which is to evacuate autonomous and indistinguishably conveyed gaussian noise. The **Daubechie 4 wavelet** method is used in order to remove the noise. It provides excellent performance in image compression. It has four wavelet and scaling function coefficient.

The Daubechie 4wavelet limit denoising involves the following steps:

1. First step involves computation of the wavelet transform of the Mammogram noisy image.
2. Second step is used to apply thresholding on noisy wavelet coefficients.
3. Finally computing inverse wavelet transform of modified wavelet coefficients.

### **Thresholding**

The purpose of thresholding is to extract those pixels from some image which represent an object (either text or other line image data such as graphs, maps). Though the information is binary the pixels represent a range of intensities. In this project for mammograms, thresholding usually involves selecting a single gray level value from an analysis of the grey-level histogram, to segment the histogram into background and breast tissues. All the pixels with grey level value less than the threshold are marked as background and the rest as breast Thresholding uses only grey level value and no spatial information is considered .Therefore, the major shortcoming of the threshold is that there is often an overlap between grey levels of the objects in the breast and the background. Hard and Soft thresholdingare taken into the considerations.

### **Hard Thresholding**

Hard thresholding is a “keep or kill” procedure and is more intuitively appealing. The choice of the threshold is a very delicate and important statistical problem. Hard thresholdingsets

any coefficient less than or equal to the threshold to zero. The formula for hard thresholding is given by,

$$\tilde{w}_{j,k} = \begin{cases} w_{j,k} & |w_{j,k}| \geq \lambda \\ 0 & |w_{j,k}| < \lambda \end{cases}$$

where  $\lambda$  is the threshold.

### Soft Thresholding

Soft thresholding shrinks coefficients above the threshold in absolute value. Soft thresholding not only smooths the time series, but moves it toward zero. The formula for soft thresholding is given by,

$$\tilde{w}_{j,k} = \begin{cases} \text{sgn}(w_{j,k})(|w_{j,k}| - \lambda) & |w_{j,k}| \geq \lambda \\ 0 & |w_{j,k}| < \lambda \end{cases}$$

## 2.2 IMAGE ENHANCEMENT

Image enhancement is fundamentally enhancing the interpretability or impression of data in pictures for human viewers and giving better contribution for other mechanized picture handling procedures [1]-[5]. The central goal of image enhancement is to change parameters of a picture to make it more appropriate for a given errand.

### 2.2.1 Create Negative of an Image

The most essential and straightforward operation in computerized image enhancement is to process the negative of a picture [7]. The pixel dim qualities are altered to register the negative of a picture. It can be seen that each pixel esteem from the first picture is subtracted from the 255. The resultant picture gets to be negative of the first picture. Negative pictures are valuable for improving white or dim detail installed in dim districts of a picture.

### 2.2.2 Logarithmic Transformations

The general type of the log change is

$$\mathbf{S} = \mathbf{C} * \log(\mathbf{1} + \mathbf{r}) \quad (1)$$

The log change maps a restricted scope of low information dark level qualities into a more extensive scope of yield qualities. The opposite log change plays out the inverse change. Log capacities are especially helpful when the info dim level qualities may have an amazingly huge scope of qualities.

### 2.2.3 Power -Law Transformations

The nth power and nth root bends can be given by the expression,

$$\mathbf{s} = \mathbf{c}\mathbf{r}^\gamma \quad (2)$$

This change capacity is additionally called as gamma amendment. For different estimations of  $\gamma$  distinctive levels of upgrades can be gotten. This system is normally called as Gamma Correction.

### 2.2.4 Wavelet-Based Texture-Characteristic Morphological Component Analysis

The wavelet-based texture-characteristic morphological component analysis (WT-TC-MCA) which has ended up being effective in improving the textural contrasts between various surfaces in gray scale picture, was connected to improve shading pictures[9]. We first exchange the picture from RGB shading space to CIELab shading space, and then the WT-TC-MCA strategy is utilized to upgrade the luminance (L) channel as a grayscale textural picture[4]. In the wake of changing over back to the RGB shading space with the improved L-channel, the shading picture is improve with more discernable surface contrasts while saving tint and perceptual impact.

The WT-TC-MCA based shading image enhancement is executed as follows:

1. Change the information picture I from RGB shading space to CIELab shading space;
2. Upgrade the L segment by the WT-TC-MCA strategy so that diverse in l channel are adjusted to be commonly more extraordinary to get the upgraded segment L;

3. Supplant the L part with L', then change the shading picture back to the RGB shading space, yielding the surface improved shading picture I.

## **2.3 IMAGE SEGMENTATION**

### **2.3.1 Dynamic Contour Models**

Chan-Vese (CV) Model at first proposed by Chan and Vese to settle the piecewise steady division issue[8]. It has been generally utilized and broadened to address an extensive variety of division issues.

Exertion has been made to adjust the CV display with the goal that it can be utilized to address more muddled issues than simply the piecewise steady issue. Channels which can improve vessel-like structures have played.

### **2.3.2 Typical Vesselness Filters**

Filters which can enhance vessel-like structures have played an important role in the vessel segmentation problems[23].

The three most influential filters are

- **Eigen value-Based Filter**

This filter is based on eigen values of the Hessian matrix For each pixel of a 2D image with intensity ,the Hessian matrix can be formed by its 3 second derivatives and from which two eigen values can be computed.

- **Isotropic Undecimated Wavelet Filter**

The isotropic undecimated wavelet transform (IUWT) has recently been used for vessel segmentation and showed good accuracy and computational efficiency. Applied to a signal , subsequent scaling coefficients are calculated by convolution with a filter.

- **Local Phase-Based Filter**

Local phase is an important local feature that can measure structural information (e.g., lines and edges) of an image. It has recently been shown that this information can be used to enhance vessels in a more precise way and produce promising segmentation results.

### **2.3.3 Mass Segmentation Algorithm**

The segmentation algorithm of a mass tissue in a digital mammogram can be divided into three sections:

- Mammogram pre-processing.
- Biased normalized cut image segmentation to delineate pectoral muscle.
- Segmentation of masses using 2-D Entropy.

### **2.3.4 Segmentation using Morphological Operation**

The thresholding method is used for detecting the pectoral muscle in the mammogram images. thepreprocessed mammogram images are thresholded by using the mid pixel value in the breast area[15]-[17]. since the mammogram images are grayscale images, they are thresholded by setting a value.

Unlike hard and soft thresholding, it converts all the pixels to either black or white. the pectoral muscle since it is a dense tissue bundle, it appears as white pixels in the thresholded image. Similarly some of the dense tissues and abnormal growth like tumor, calcification masses, etc., are displayed as white pixels.

Rest of the pixel will turn black, resulting the pectoral muscle alone in the mammogram image. This is useful for segmenting the pectoral muscle from the breast by segmentation process.

The other white pixel are removed by using connected component labeling. Each components are labeled are then they are removed using Otsu's segmentation algorithm.

Using morphological operations like complementing, subtracting, one can achieve the removal of pectoral muscle. After identifying the pectoral muscle, the image is complemented, thus resulting in making the pectoral muscle appear black and rest of the image in white. Then the complemented image is subtracted from original image. Then the resultant image gives the processed segmented image.

## **2.4. MATCHING CC AND MLO MAMMOGRAM**

### **2.4.1 De-Lau nay Triangulation**

In a 2-D point set, the Delaunay triangulation can be performed. Three points form a valid triangle if the following condition is met [41].

1. The circumcircle of the triangle must not contain any other points from the point set (points are allowed to be on the rim of the circumcircle).
2. The Delaunay triangulation is not necessarily uniquely defined and might not be defined at all. e.g. for points lying on a straight line.

The dual graph of a 2-D Delaunay triangulation connects the centers of the circumscribing circles to a new diagram called the Voronoi diagram or Voronoi tessellation. Several algorithms exist for the creation of both Delaunay triangulations and Voronoi tessellations. Voronoi tessellations can be created using the Bowyer- Watson algorithm.

### **2.4.2 K-D Tree**

A K-d tree, or K-dimensional tree, is a data structure used in computer science for organizing some number of points in a space with k dimensions [41]. It is a binary search tree with other constraints imposed on it. K-d trees are very useful for range and nearest neighbor searches. For our purposes we will generally only be dealing with point clouds in three dimensions, so all of our K-d trees will be three-dimensional. Each level of a K-d tree splits all children along a specific dimension, using a hyperplane that is perpendicular to the corresponding axis. At the root of the tree all children will be split based on the first dimension (i.e. if the first dimension coordinate is less than the root it will be in the left-sub tree and if it is greater than the root it will obviously be in the right sub-tree). Each level down in the tree divides on the next dimension, returning to the first dimension once all others have been exhausted. The most efficient way to build a k-d tree is to use a partition method like the one Quick Sort uses to place the median point at the root and everything with a smaller one dimensional value to the left and larger to the right. Then repeat this procedure on both the left and right sub-trees until the last trees that is to partition are only composed of one element.

## 2.5. 3D RECONSTRUCTION

### 2.5.1. SIFT (Scale Invariant Feature Transform)

The SIFT algorithm takes an image and transforms it into a collection of local feature vectors[26]. Each of these feature vectors is supposed to be distinctive and invariant to any scaling, rotation or translation of the image. In the original implementation, these features can be used to find distinctive objects in different images and the transform can be extended to match faces in images. Our method is implemented as the following stages:

- Creating the Difference of Gaussian Pyramid
- Extrema Detection
- Noise Elimination
- Orientation Assignment
- Descriptor Computation
- Keypoints Matching.

#### Creating the Difference of Gaussian Pyramid

The first stage is to construct a Gaussian "scale space" function from the input image. This is formed by convolution (filtering) of the original image with Gaussian functions of varying widths.

#### Extrema Detection

This stage is to find the extrema points in the DOG pyramid. To detect the local maxima and minima of  $D(x, y, \sigma)$ , each point is compared with the pixels of all its 26 neighbours. If this value is the minimum or maximum this point is an extrema. We then improve the localisation.

#### Noise Elimination

This stage attempts to eliminate some points from the candidate list of keypoints by finding those that have low contrast or are poorly localised on an edge.

## **Orientation Assignment**

This step aims to assign a consistent orientation to the keypoints based on local image properties. An orientation histogram is formed from the gradient orientations of sample points within a region around the keypoint.

## **Descriptor Computation**

In this stage, a descriptor is computed for the local image region that is as distinctive as possible at each candidate keypoint. The image gradient magnitudes and orientations are sampled around the keypoint location. These values are illustrated with small arrows at each sample location on the first image of Figures. A Gaussian weighting function with  $\sigma$  related to the scale of the keypoint is used to assign a weight to the magnitude. We use a  $\sigma$  equal to one half the width of the descriptor window in this implementation. In order to achieve orientation invariance, the coordinates of the descriptor and the gradient orientations are rotated relative to the keypoint orientation.

## **Keypoints Matching**

In this stage, some matching tests are running to test the repeatability and stability of the SIFT features. The features of the two images are computed separately. Then each keypoint in the original image (model image) is compared to every keypoints in the transformed image using the descriptors computed in the previous stage. We can currently calculate the SIFT features for an image and have experimented with some simple matching schemes between images. Noise adjustment is a very essential part for our approach which could result in inefficient or false matching. However, we have used parameters which should help the keep the feature matching robust to noise in this implementation.

### **2.5.2. ICP (Iterative Closest Point) Algorithm**

The ICP algorithm iteratively performs the following steps[32].

- For every data point the nearest neighbor in the model point set is found.
- The error metric is minimized.
- Data points are transformed using the minimization result.

It identifies six distinct stages of the algorithm:

### **Selection**

- This stage selects samples that constrain all degrees of freedom of the rigid-body transformation

### **Matching**

- This stage matches the correspondence points with the rotation and translation parameter.

### **Weighting**

- This stage weighs the correspondence pairs.

### **Rejecting**

- This stage rejects certain (outlier) point pairs. Corresponding points with point to point distance will be higher than a given threshold.

### **Error metrics**

- Sum of squared distances from each sample point to the plane containing the destination point (Point to Point) will be calculated as error metrics.

### **Minimization of error metric**

- Repeatedly generating set of corresponding points using the current transformations and finding new transformations will minimize the error metric.

Matching is of three types:

- 1) Brute force triangulation
- 2) Delaunay triangulation
- 3) K d tree Matching

### 2.5.3 Affine Reconstruction from Multiple Views using Singular value Decomposition

The advantage of having a projective transformation is to be able to view the scene in perspective [46]. In simple terms, an affine transformation is a non-singular linear transformation which undergoes a translation.

Once an object is affine transformed, there are three geometric properties that remain invariant of the transformation. They are as follows

- Parallel lines

A pair of parallel lines in the 3D world has a vanishing point at infinity. Under affinity, this vanishing point would still be mapped to another point at infinity. This means that After the affine transformation, the lines must remain parallel for them to have a vanishing point at infinity. Therefore, parallel lines remain parallel after an affine transformation.

- Ratio of lengths of directional lines

Lines that are placed in the same direction contain a ratio that is invariant. It implies that the ratios of two lengths along parallel lines remain invariant and the ratio of two lengths that are not parallel is not invariant.

- Ratio of areas

As parallel lines remain parallel after an affine transformation, the ratios of surface areas remain invariant. This builds on from the second invariant because the directional ratios of lengths determine the area and two areas would therefore have the same ratio. The invariants of affine transformation highlight the importance of affine geometry.

## **CHAPTER 3**

### **IMAGE DATABASE**

Two image databases are used for this work. They are

1. DDSM
2. INBREAST

#### **3.1 DDSM**

The Digital Database for Screening Mammography (DDSM) is a database of digitized filmscreen mammograms with related ground truth and other data. The motivation behind this asset is to give a substantial arrangement of mammograms in an advanced organization that might be utilized by scientists to assess and analyze the execution of PC supported identification (CAD) calculations. The database was finished in the fall of 1999. It contains 2620, four view, mammography screening exams. Since that time, the database has been upgraded through the expansion of new programming devices that disentangle the extraction of picture information. Other document designs, permit streamlined access to the information in the ground truth records and rearrange the means important to assess a CAD calculation.

#### **3.2 INBREAST DATABASE**

The database was gathered at the Breast Center of Hospital São João, Porto, under authorization of the Hospital's morals advisory group. Pictures were obtained between April 2008 and July 2010. The securing hardware was the MammoNovation Siemens, with a Solid-state finder of undefined selenium, with a pixel size of 70mm (microns), and 14bit differentiation determination. The picture network was 33284084 or 25603328 pixels, contingent upon the pressure plate utilized as a part of the obtaining (as per the bosom size of the patient). Pictures were spared in the Digital Imaging what's more, Communications in Medicine (DICOM) format. All private data was evacuated from the DICOM record, as indicated by Supplement 55 of the DICOM standard. The correspondence between pictures

of a similar patient is kept with an arbitrarily created Patient ID. INbreast has FFDM pictures from screening, demonstrative and follow-up cases. Screening is made by national and territorial principles (Lee et al., 2010). Finding is made when the screening hints at irregularity. In follow-up pictures, growth was already distinguished and treated. A sum of 115 cases were gathered, of which 90 have 2 pictures (MLO and CC) of every bosom and the rest of the 25 cases are from ladies who had a mastectomy, and in this way just 2 perspectives of one bosom were incorporated. This wholes to an aggregate of 410 pictures. 8 of the 90 cases with 2 pictures for every bosom additionally have pictures obtained in various timings.

The database includes examples of normal mammograms, mammograms with masses, mammograms with calcifications, architectural distortions, asymmetries, and images with multiple findings and their BI-RADS rating. BI-RADS is an acronym for Breast Imaging-Reporting and Data System, a quality assurance tool originally designed for use with mammography.

BI-RADS Assessment Categories are:

Category 0: Incomplete

Category 1: Negative

Category 2: benign findings;

Category 3: probably benign findings;

Category 4: suspicious findings;

Category 5: a high probability of malignancy; and

Category 6: proved cancer

In case of categories 4 and 5, a biopsy is needed to exclude or confirm malignancy.

## CHAPTER 4

### PROPOSED WORK

The first step of the proposed work includes the collection of MLO and CC view mammograms of DDSM data bases and preprocessing them. In the second step, the images are preprocessed by noise removal and image enhancement. In the third step, pectoral muscle should be segmented. In the fourth step, the segmented tumor from the mammogram is 3D reconstructed in order to find the exact location of the tumor growth.

#### 4.1 PROPOSED WORK DIAGRAM

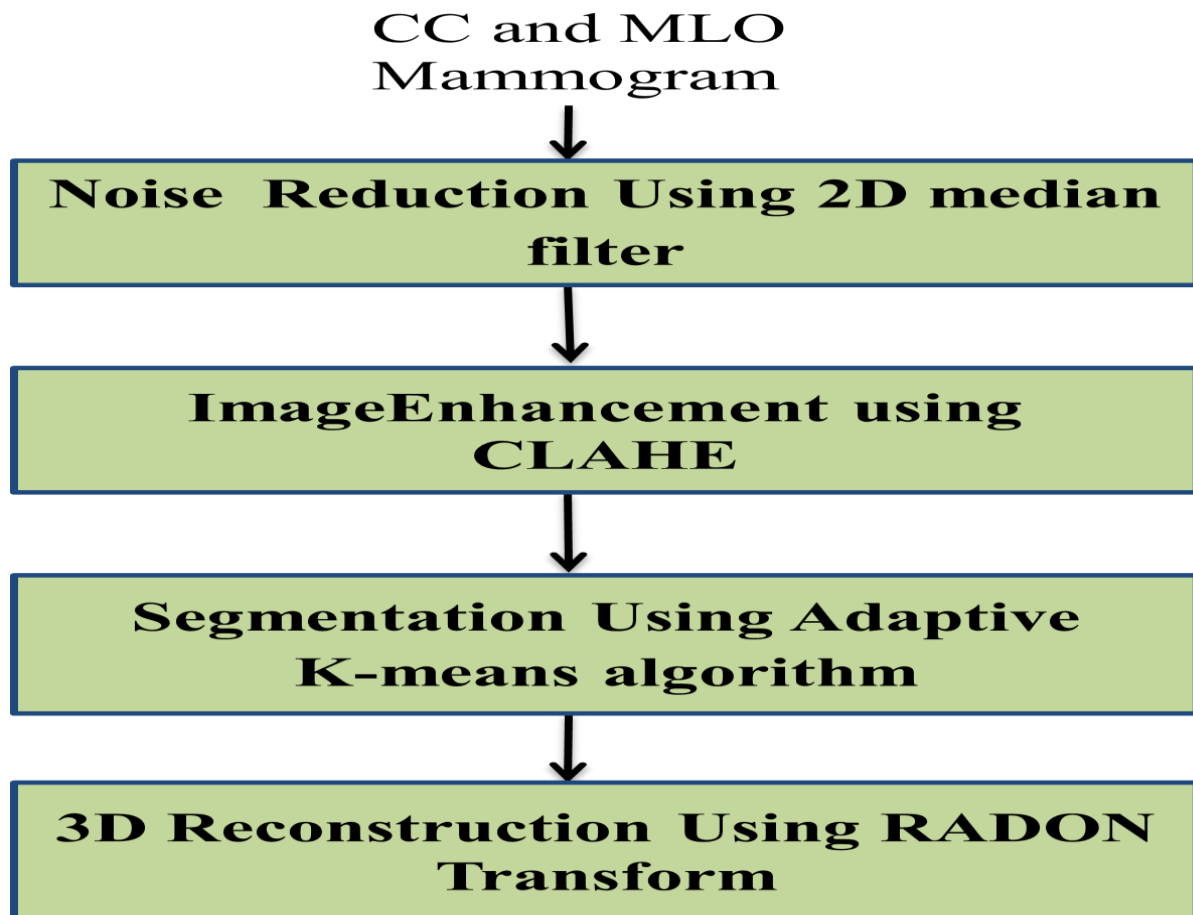


fig 4.1 Proposed work diagram

## 4.2 NOISE REDUCTION

Median filtration is one of the most popular methods of noise removal [43]. It is especially useful in case of enhancement of images corrupted by impulse. Applied to grayscale images, median filtration is a neighborhood brightness-ranking algorithm. Each pixel is equal to the median intensity of its closest neighborhoods in the original image. The size of the neighborhood is determined by the mask, which passes through the image row-by-row (or column-by-column).

Moreover, it is commonly used in many practical applications of vision systems as a part of image enhancement process. It is much more robust in impulse noise removal than the traditional linear filtering, because it preserves the sharp edges.

The main stages of the proposed algorithm to impulse noise removal are:

- Each M by N matrix of the image pixel under subject is analyzed for its median value by a window which slides through the image.
- Then the center of each window sliding matrix is replaced by its median value.
- By default, the size of the window is 3 x 3 matrix.
- Finally, output pixel contains the median value in the M-by-N neighbourhood around the corresponding pixel in the input image.

## 4.3 IMAGE ENHANCEMENT

### 4.3.1 Histogram Equalisation

Histogram equalization (HE) is a modeling strategy which maps the information dim levels to a bright level corresponding to its aggregate thickness and consequently, the likelihood of every dim level in coming about picture is consistently circulated [12]. The yield picture histogram ought to preferably contain an equivalent number of pixels at each discrete dim level esteem. The histogram adjustment strategy is worldwide and daze with the end goal that it doesn't include visual detail into record while upgrading the picture. It brings about over the top differentiate upgrade, which causes the unnatural look and visual relics of the handled picture

Histogram equalization frameworks are utilized to bind the change rate. HE reshape the information histogram by diminishing or expanding the value in the histogram bins predicated on

an edge confine up to the alteration is happening. The histogram will be cut predicated on this edge regard. From time to time cut part will be redistributed afresh to the histogram and a short time later histogram leveling is finished. Histogram Equalization (HE) is much a greater number of more useful for intricacy updated.

### **4.3.2 Contrast Limited Adaptive Histogram Equalisation(CLAHE)**

CLAHE is a variant of adaptive histogram equalization. It divides the original image into several non overlapping sub images [22]. Histogram of the sub images are clipped to limit the amount of enhancement of each pixel and then equalized. The details in the image appear clearly relative to the background. The same time the background of image is enhanced equally as the foreground of the image which leads to the high contrast output image. The brightness is maintained throughout the process.

## **4.4 IMAGE SEGMENTATION**

### **4.4.1 Adaptive K-Means Clustering**

Adaptive K-Means clustering is a rather simple but well known algorithm for grouping objects, clustering [44]. Again all objects need to be represented as a set of numerical features. In addition the user has to specify the number of groups (referred to as  $k$ ). Each object can be thought of as being represented by some feature vector in an  $n$  dimensional space,  $n$  being the number of all features used to describe the objects to cluster.

The algorithm then randomly chooses  $k$  points in that vector space, these points serve as the initial centres of the clusters. Afterwards all objects are each assigned to the centre they are closest to. Usually the distance measure is chosen by the user and determined by the learning task.

After that, for each cluster a new centre is computed by averaging the feature vectors of all objects assigned to it. The process of assigning objects and recomputing centres is repeated until the process converges. The algorithm can be proven to converge after a finite number of iterations. Several tweaks concerning distance measure, initial centre choice and computation of new average centres have been explored, as well as the estimation of the number of clusters  $k$ . Yet the main principle always remains the same.

Adaptive k-means clustering is a method of vector quantization, originally from signal processing, that is popular for cluster analysis in data mining. Adaptive k-means clustering aims to partition  $n$  observations into  $k$  clusters in which each observation belongs to the cluster with the nearest mean, serving as a prototype of the cluster.

In the Adaptive k-mean algorithm, the number of elements in each cluster is stochastic. It is possible that some groups own a large proportion of elements while others just possess a few of them. However, in some situations, the proportion of elements in each cluster need to be controlled so as to make the distribution of elements satisfied.

### **Algorithm**

The adaptive K-means clustering algorithm starts with the selection of  $K$  elements from the input data set. The  $K$  elements form the seeds of clusters and are randomly selected. The properties of each element also form the properties of the cluster that is constituted by the element. The algorithm is based on the ability to compute distance between a given element and a cluster. This function is also used to compute distance between two elements.

An important consideration for this function is that it should be able to account for the distance based on properties that have been normalized so that the distance is not dominated by one property or some property is not ignored in the computation of distance. In most cases, the Euclidean distance may be sufficient. It should be pointed out that for performance reasons, the square root function may be dropped. In other cases, we may have to modify the distance function. Such cases can be exemplified by data where one dimension is scaled different compared to other dimensions, or where properties may be required to have different weights during comparison.

With the distance function, the algorithm proceeds as follows: Compute the distance of each cluster from every other cluster. This distance is stored in a 2D array as a triangular matrix. We also note down the minimum distance  $d_{min}$  between any two clusters  $C_{m1}$  and  $C_{m2}$  as well as the identification of these two closest clusters.

The algorithm includes the following steps:

- Vectorise all data.

- Initialize iteration count (i=0, j=0).
- Find data points. Data point= mean(data)
- Initialize data point , increment count for each iteration(i=i+1).
- Find distance between data and data points.

$$Dist = \sqrt{(data - data\ points)^2} (3)$$

- Find bandwidth for each cluster center.

$$BW = \sqrt{(\sum \frac{(data - data\ points)^2}{numel(data)})} \quad (4)$$

- The qualified bandwidth is selected based on

$$Distance < bandwidth (5)$$

- The new data points are found by

$$new\ data\ point = mean (new\ data) \quad (6)$$

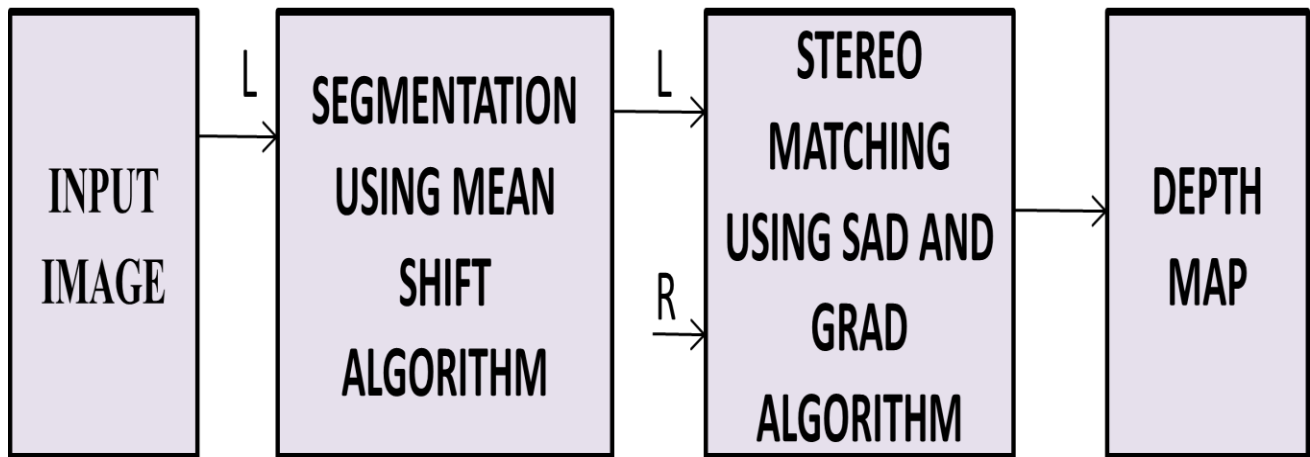
- Store center of cluster.
- Check maximum number of cluster.
- Sort center.
- Find the difference between two consecutive center.
- Find minimum distance between two cluster center.
- Discard cluster center less than distance.

In the adaptive K-means algorithm, the number of elements in each cluster decides the number of comparisons for each search. Since there are K clusters, we have to perform K comparisons to find the most promising cluster for further exploration. In the worst case, all the clusters except one are single-element clusters. If the cluster with N-K elements is selected for further exploration, the algorithm performs K comparisons to get the appropriate cluster, and N-K comparisons to look for the appropriate element within that cluster.

Thus, the algorithm results in O(N) comparisons which makes it perform just like linear search. In the best case, the data elements are distributed uniformly across clusters. In such a case, each cluster contains N-K elements. A search in this case will take at most K comparisons to determine the appropriate cluster, and N=K comparisons to determine the appropriate element.

## 4.5 DEPTH MAP ESTIMATION

Obtaining a precise and accurate depth map is the ultimate goal for 3D image reconstruction [45]. This chapter is focused on the process of the depth map estimation from the mammograms that are captured by the detector placed in such positions so that the breast is taken from two slightly different views (angles). By using modern stereo vision systems, we can accurately estimate the depth. A large number of algorithms have been proposed to solve this problem. However an assignment of the stereo matching algorithm is used to find corresponding points in both images that represent the same scene point by using the combination of SAD(Sum Of Differences) and GRAD(Gradient Of Differences).



L – CC Mammogram

R – MLO Mammogram

fig 4.2 Depth Map Estimation Block Diagram

### 4.5.1 Mean Shift Segmentation

The mean shift algorithm is a non parametric iterative clustering technique which does not require prior knowledge of the number of clusters and does not constrain the shape of the clusters.

To find local maxima of the probability density (density modes) given by samples.

- Start with a random region of interest.
- Determine a centroid of the data.
- Move the region to the location of the new centroid.
- Repeat until convergence.

The algorithm is based on the kernel density estimation. Let a set of  $d$ -dimensional data points is represented by values  $x_i$ ,  $i = 1, 2, \dots, n$  in  $d$ -dimensional space  $R_d$ . The number of points  $x_i$  belonging to  $d$ -dimensional area around  $x$  with edge length  $h$  is given by:

$$\hat{f}_{h,K} = \frac{1}{nh^d} \sum_{i=1}^n K\left(\frac{x - x_i}{h}\right) \quad (7)$$

where  $h$  defines the radius of kernel and  $K(x)$  is kernel or window function. Thus, the kernel density estimation is given by:

$$\nabla \hat{f}_{h,K}(x) = \frac{2c_{k,d}}{nh^{d+2}} \left( \sum_{i=1}^n g_i \right) \left( \frac{\sum_{i=1}^n x_i g_i}{\sum_{i=1}^n g_i} - x \right). \quad (8)$$

A new kernel is defined as  $G(x) = c_{k,d}g(\|x\|^2)$ , where  $g(x) = -k'(x)$  is new kernel function and  $c_{k,d}$  is normalized constant.

$$m_{h,g}(x) = \frac{\sum_{i=1}^n x_i g\left(\left\|\frac{x - x_i}{h}\right\|^2\right)}{\sum_{i=1}^n g\left(\left\|\frac{x - x_i}{h}\right\|^2\right)} - x. \quad (9)$$

The Mean Shift algorithm is based on iterative computing of the mean shift vector and consistently actualizing kernel's position by equation  $x^{k+1} = x^k + m(x^k)$ .

Compute the distance of each cluster from every other cluster. This distance is stored in a 2D array as a triangular matrix. We also note down the minimum distance  $d_{min}$  between any two clusters  $C_{m1}$  and  $C_{m2}$  as well as the identification of these two closest clusters.

### 4.5.2 Stereo Matching Algorithm

A reconstruction of the disparity map from the left and right stereo pair is known as the stereo matching algorithm. The detected feature points must be matched. There exist several matching techniques based on various algorithms like SAD (Sum of Absolute Difference) and GRAD (Gradient of Absolute Difference) algorithm. The SAD algorithm is one of the simplest of dissimilarity measures of the left and right stereo images corresponding with square windows.

#### SAD (Sum of Absolute Difference) Algorithm

It computes the intensity differences for each center pixel  $(i, j)$  in a window  $W(x, y)$  as follows:

$$SAD = \sum_{(i,j) \in W(x,y)} |I_L(i, j) - I_R(i, j)| \quad (10)$$

where  $I_L$  and  $I_R$  are pixel intensity functions of the left and right image, respectively.  $W(x, y)$  is square window that surrounds the position  $(x, y)$  of the pixel. The disparity SAD( $x, y, d$ ) calculation is repeated within the  $x$ -coordinate frame in the image row, defined by zero and maximum possible disparity  $d_{max}$  of the searched 3D scene. The minimum difference value over the frame indicates the best matching pixel, and position of the minimum defines the disparity of the actual pixel. Quality of 3D disparity map depends on square window size, because a bigger window size corresponds to a greater probability of correct pixel disparity calculated from matched points, although the calculation gets slower.

#### GRAD (Gradient Of Absolute Difference) Algorithm

It computes the gradient of intensity differences for each center pixel  $(i, j)$  in a window  $W(x, y)$ . In stereo correspondence, the target is to find matching pixels of two given input images and the result from finding matching pixels is normally saved in a disparity map. The term disparity can be looked upon as horizontal distance between two matching pixels and the disparity map defines a value of this horizontal pixel distance for each image pixel coordinate. Hence, it may be seen as a function of image pixel coordinates. The left and right images of a stereo pair are sometimes denoted as reference image and search image. The reference image is defined by which view the disparity map is generated for.

## Cost of SAD AND GRAD Algorithm

In order to find corresponding pixels in a search and reference image, there is obviously a need for a pixel similarity measure. It is however more common to use the term dissimilarity measure or matching cost, which increases as the similarity between two compared pixels decreases.

A common notation for representing matching cost is through a function of reference image coordinates and disparity. The cost function returns the value of the dissimilarity for a coordinate in the disparity space. The disparity space is made up by the available image pixel coordinates and the disparity search range. Normally, a disparity search range has to be specified manually and depends upon the characteristics of the input image pair. The cost of SAD and GRAD value is obtained by

$$\text{CSAD} = W * \text{FILTER}(\text{SAD})$$

$$\text{CGRAD} = W * \text{FILTER}(\text{GRAD VALUE})$$

where W is the weight of SAD and GRAD value.  $w=3$ ,

$$\text{DISPARITY} = \text{CSAD} + \text{CGRAD}$$

### Algorithm

- Assign window size.
- Determine pixel correspondence from R(MLO) and L(CC segmented image).
- For determining the pixel correspondence, the window slides across each pixel from R to L.
- By sliding the window, the disparity and the minimum difference between the pixel correspondence are found.
- Then the gradient of each pixel in L and R are found.
- Similarly for determining the pixel correspondence from L to R, the image is shifted.
- Then the negative values of disparity and minimum difference is made absolute to produce positive values.
- Find the sum of SAD value and GRAD value.
- Get all the disparity values.

- Check all boundaries and check for infinity in disparity values and assume it as “not a number”.
- Move disparities and minimum differences to the right spot.
- Find the best match between the pixel correspondence.

#### 4.6 3D RECONSTRUCTION OF TUMOR FROM MAMMOGRAM

3D information plays an increasing role in today's medical imaging for the benefits of both diagnosis and therapy [39]. However if 3D is routinely used in the field of bone or soft tissue imaging, it is still an emerging technique in the mammography domain. The main reason is that the gold standard method for mammographic imaging. The tumour identified from mammogram can be reconstructed by using radon transform.

The radon transform gives the projection of the image intensity along a radial line oriented at a specific angle ( $\Theta$ ). Each projection can be considered as the cross section of the data in that region which was subjected to radon transform.

With the projections, the data can be reconstructed to 3D form by using inverse transform with filtered back projection algorithm.

##### 4.6.1 Radon Transform

The Radon transform is the projection of the image intensity along a radial line oriented at a specific angle ( $\Theta$ ). The Radon transform is a mapping from the Cartesian rectangular coordinates  $(x,y)$  to a distance and an angle  $(r,q)$ , also known as polar coordinates.

The disparity image obtained from depth map estimation is projected along the radial lines at different angles. each angle produces a projection or cross section of that region.

The projection can be given by,

$$P_e(t) = \int_{(\theta,t)line} f(x,y) ds \quad (11)$$

The radon transform is given by,

$$R(\rho, \theta) = \iint_{-\infty}^{\infty} f(x,y) \delta(\rho - x \cos \theta - y \sin \theta) dx dy \quad (12)$$

## 4.6.2 Inverse Radontransform

The algorithm known as the filtered back projection algorithm is presently the optimum computational method for reconstructing a function from knowledge of its projections. This algorithm can be considered as an approximate method for computer implementation of the inversion formula for the Radon transform. Unfortunately, there is a confusion associated with the name, because the filtering of the projections is done before the back projection operation. This Filtered Back projection formula for computing the inverse Radon transform implies that the parameter domain is altered with the absolute frequency in the y direction for all values of x and then the back projection part integrates up along a line. the linear expression in the back projection integral is like the one found with the point source i.e., the point sources by the Radon transform been spread into the parameter domain.

The projected radon transformed disparity image is reconstructed using the the filtered back projection. This is called as the 3D reconstructed tumor image.

## 4.7 PERFORMANCE MEASURES OF IMAGE ENHANCEMENT

### 4.7.1 Mean Square Error

The mean-squared error (MSE) between two images  $g(x,y)$  and  $g'(x, y)$  is:

$$e_{MSE} = \frac{1}{MN} \sum_{n=1}^{M,N} [g'(n, m) - g(m, n)]^2 (13)$$

### 4.7.2 Peak Signal to Noise Ratio

Peak Signal-to-Noise Ratio (PSNR) avoids this problem by scaling the MSE according to the image range.

$$PSNR = 10 \log_{10} \frac{S^2}{e_{MSE}} (14)$$

### 4.7.3 Structure Similarity Index Measure

SSIM is utilized for measuring the comparability between two pictures. The SSIM list is a full reference metric. The estimation or expectation of picture quality depends on an underlying uncompressed or twisting free picture as reference. SSIM is intended to enhance conventional

techniques, for example, peak signal to noise ratio (PSNR) and mean squared error (MSE), which have turned out to be conflicting with human visual observation.

$$\mathbf{SSIM} = \frac{(2\mu_x\mu_y+c_1)(2\sigma_{xy}+c_2)}{(\mu_x^2+\mu_y^2+c_1)(\sigma_x^2+\sigma_y^2+c_2)} \quad (15)$$

$\mu_x$  is the average of x,

$\mu_y$  is the average of y,

$\sigma_x$  is the variance of x,

$\sigma_y$  is the variance of y,

$\sigma_{xy}$  is the covariance of x and y,

$C_1$  and  $C_2$  are the two variables to stabilize the division with weak denominator.

## **CHAPTER 5**

### **RESULTS AND SIMULATION**

#### **5.1 NOISE REMOVAL USING ADAPTIVE MEDIAN FILTER**

The noise removal for CC and MLO mammogram has been done by adaptive median filter and the results are as follows.

#### **DENOISED CC MAMMOGRAM**

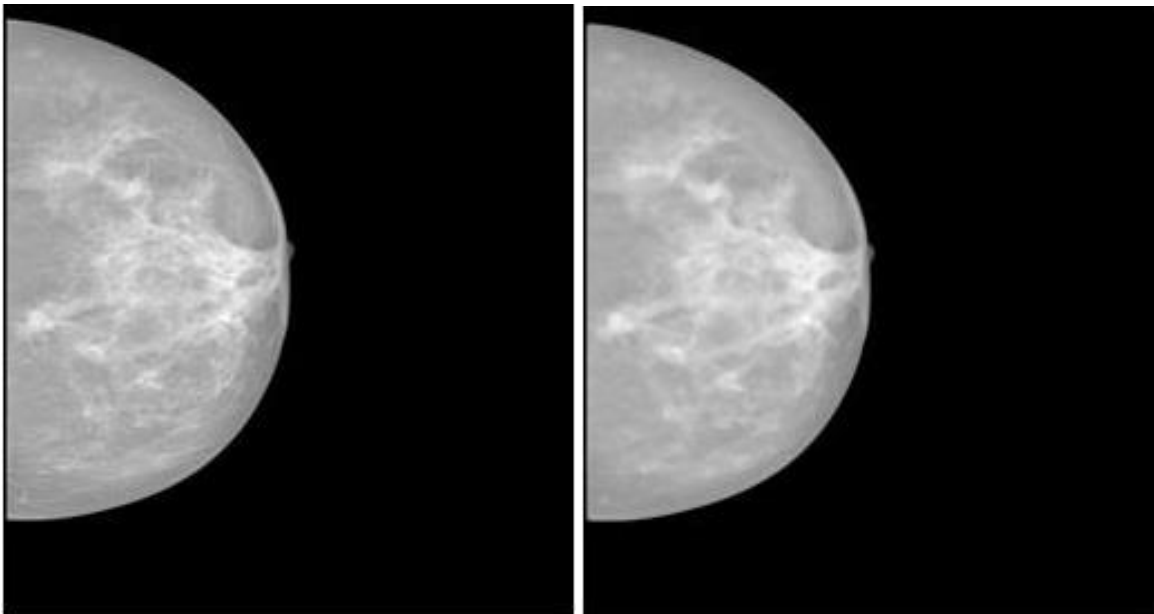


**Fig 5.1.1 (a) Original and (b) Denoised CC Mammogram**

## DENOISED MLO MAMMOGRAM

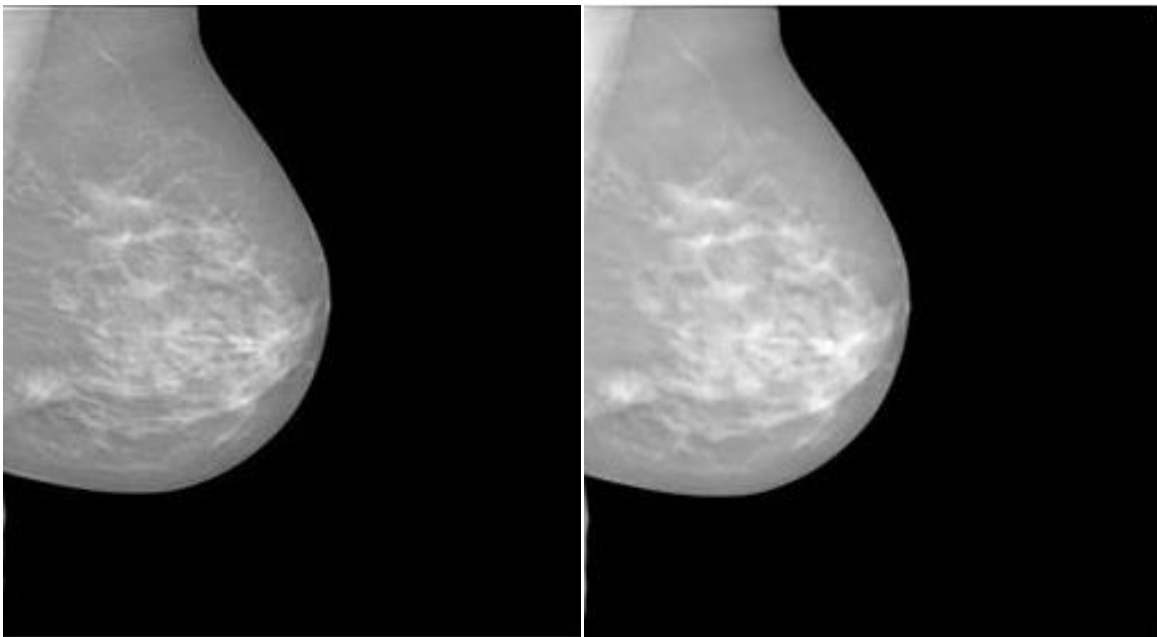
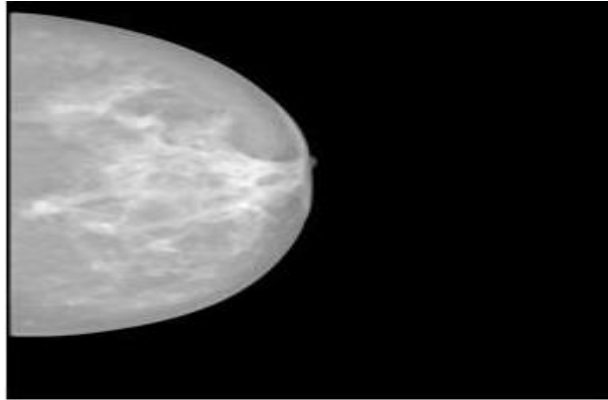


**Fig 5.1.2 (a) Original And (b) Denoised MLO Mammogram**

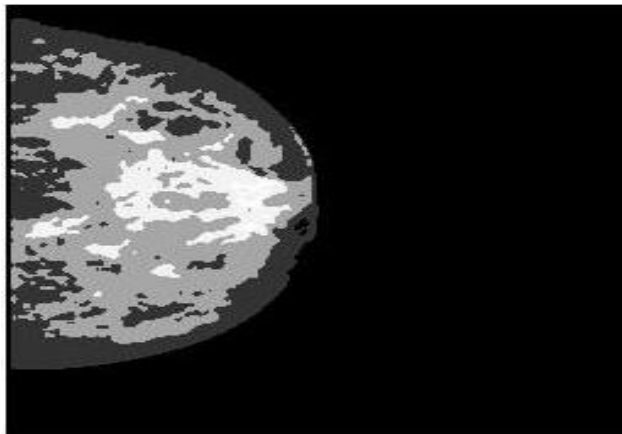
## 5.2 IMAGE ENHANCEMENT - CC MAMMOGRAM

The image enhancement for CC and MLO mammogram has been done by Contrast Limited Adaptive Histogram Equalisation and the results are as follows.

### DENOISED MAMMOGRAM



### HISTOGRAM EQUALISED MAMMOGRAM



### CLAHE ENHANCED MAMMOGRAM

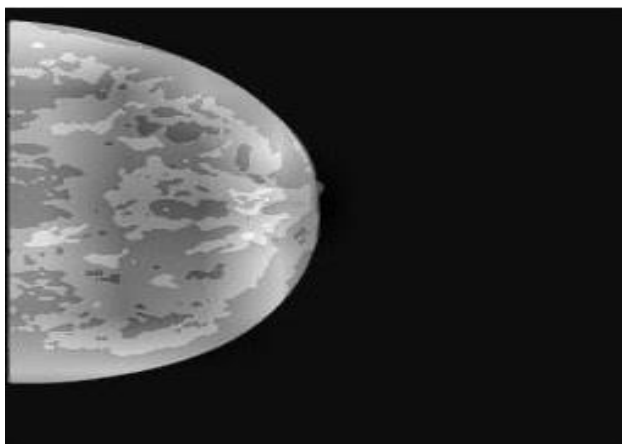
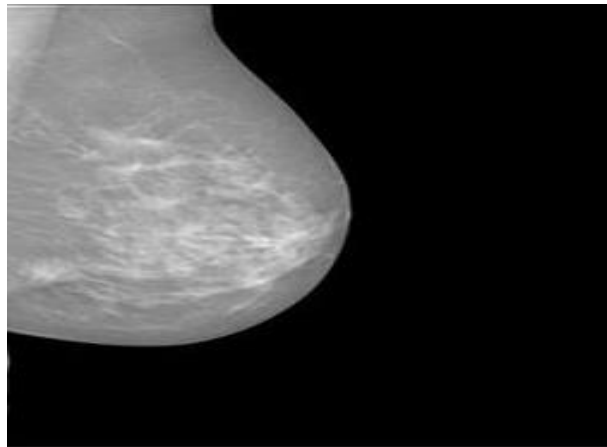


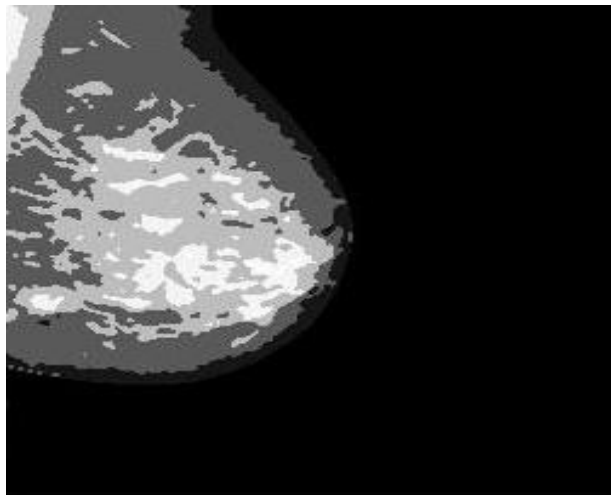
**Fig 5.1.3 Enhanced CC Mammogram using CLAHE**

## IMAGE ENHANCEMENT - MLO MAMMOGRAM

### DENOISED MAMMOGRAM



### HISTOGRAM EQUALISED MAMMOGRAM



### CLAHE ENHANCED MAMMOGRAM

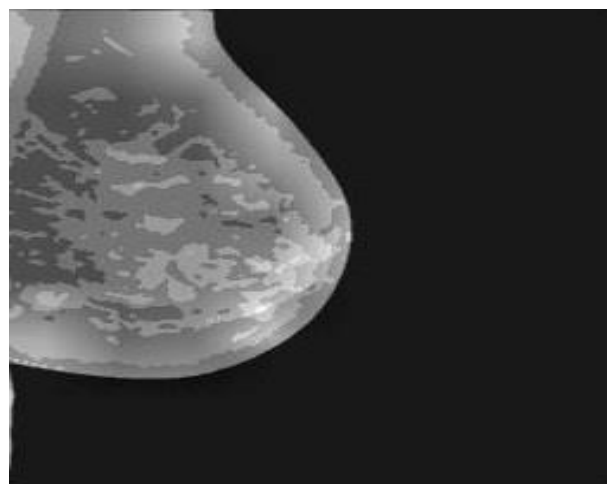
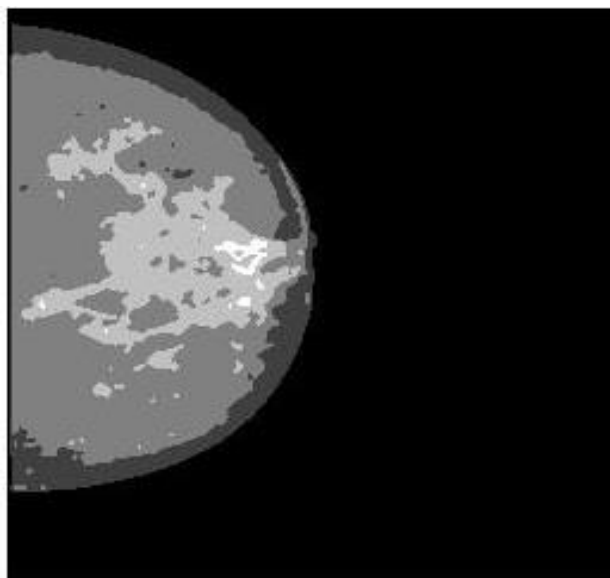


Fig 5.1.4 Enhanced MLO Mammogram using CLAHE

### **5.3IMAGE SEGMENTATION - CC MAMMOGRAM**

The segmentation for CC and MLO mammogram has been done by Adaptive K- means clustering and the results are as follows.

#### **CLUSTEREDMAMMOGRAM**



#### **TUMOUR SEGMENTED**

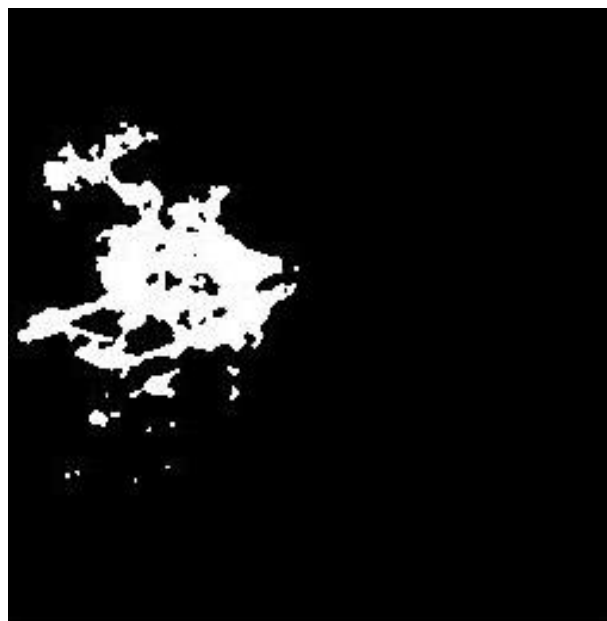
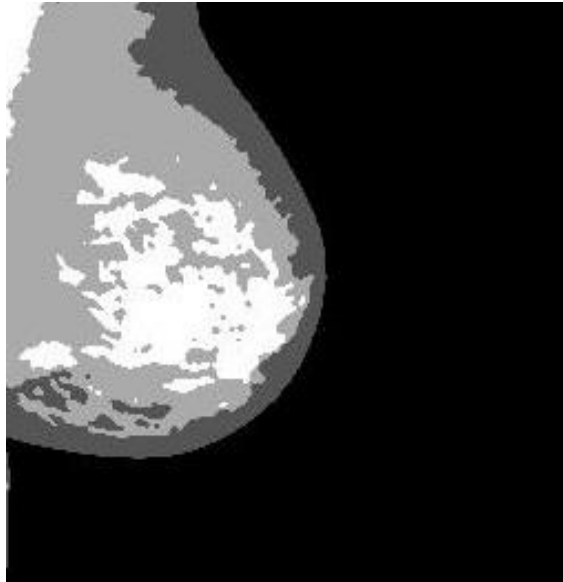


**Fig 5.1.5 Clustered Mammogram and Segmented Tumour from CC Mammogram**

## IMAGE SEGMENTATION -MLO MAMMOGRAM

### CLUSTEREDMAMMOGRAM



### TUMOUR SEGMENTED

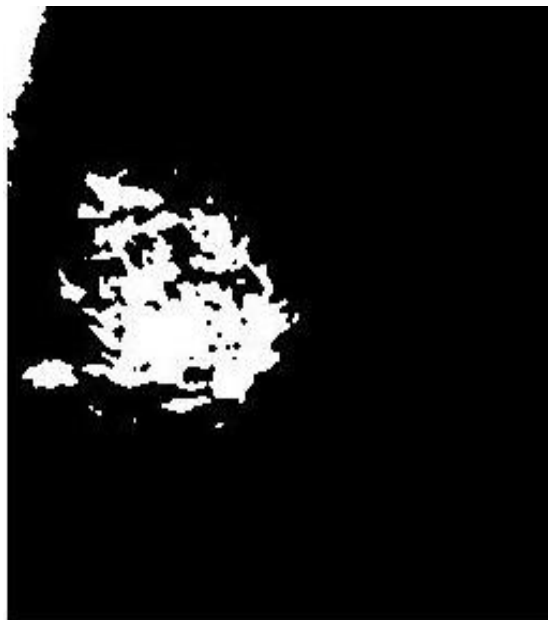


**Fig 5.1.6 Clustered Mammogram and Segmented Tumour from MLO Mammogram**

#### **5.4 CLUSTERED CC -TUMOUR USING MEAN SHIFT ALGORITHM**

The tumor from CC view is segmented again by mean shift algorithm and the results are as follows.



**Fig 5.1.7 Clustered Tumour using Mean Shift Segmentation Algorithm**

## 5.5 DEPTH MAP OF CC AND MLO VIEW MATCHED IMAGE

The depth map is estimated using stereo matching algorithm to match the CC and MLO mammogram and the results are as follows

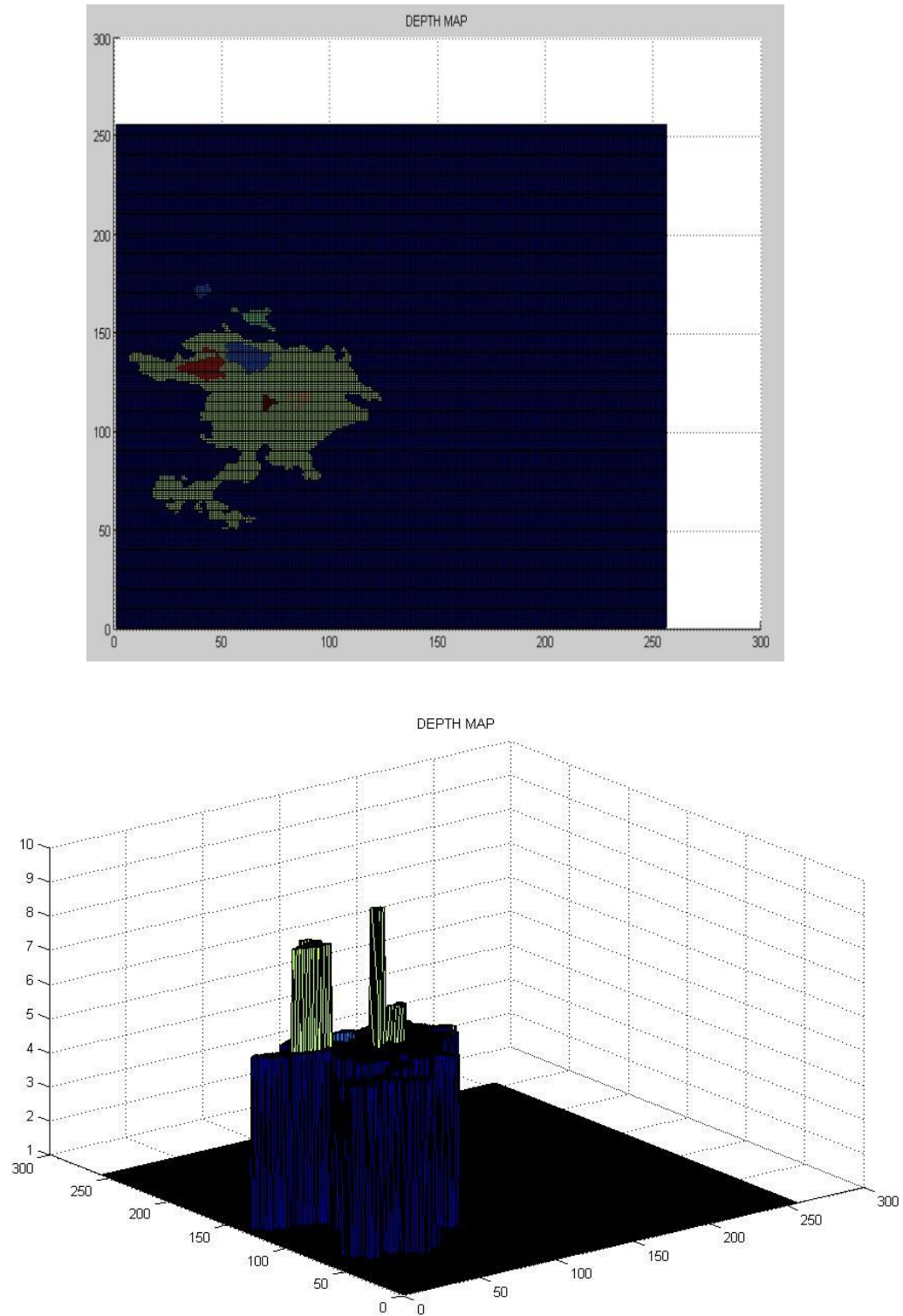


Fig 5.1.8. Depth map of CC and MLO view matched image

## 5.6 RECONSTRUCTION USING 4 PROJECTIONS

The radon and inverse radon transform is taken for the tumor in 4 projections and the results are as follows

### Radon Transform of Tumor

radon



### Inverse Radon Transform of Tumour

3D IMAGE

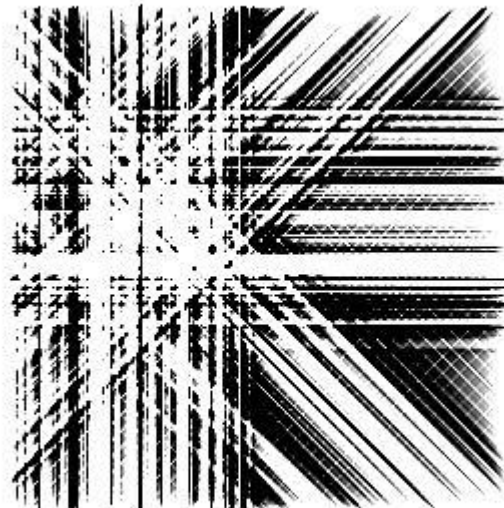
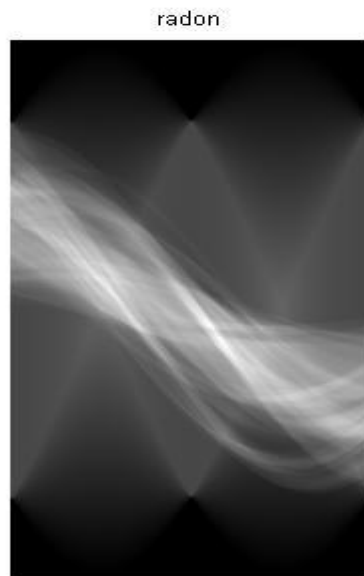


Fig 5.1.9.Reconstruction using 4 Projections

## 5.7 RECONSTRUCTION USING 180 PROJECTIONS

The radon and inverse radon transform is taken for the tumor in 180 projections and the results are as follows

### Radon Transform of Tumor



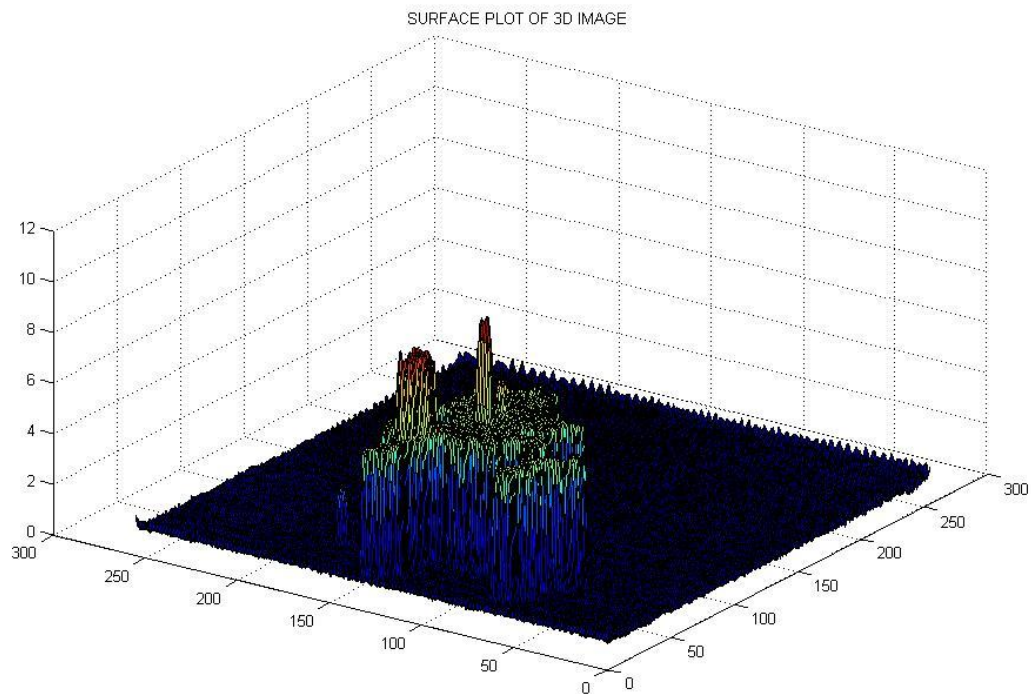
### Inverse Radon Transform of Tumour



Fig 5.1.10.Reconstruction using 180 Projections

## 5.8 SURFACE PLOT OF 3D RECONSTRUCTED TUMOR

The surface plot of 3D reconstructed tumour is used for finding the exact location of the tumor and the results are as follows,



**Fig 5.1.11. Surface Plot of 3D Reconstructed Tumour**

## 5.9 PERFORMANCE MESURES FOR PRE-PROCESSING

Peak signal to noise ratio values for various mammogram images:

<b>HISTOGRAM EQUALISATION</b>	<b>CLAHE</b>
11.5983	15.3254
11.8962	15.9685
11.384	15.206
11.853	15.8956
10.864	14.862
10.956	15.0598
10.465	14.5689

Structure similarity index measure for various mammogram images:

<b>HISTOGRAM EQUALISATION</b>	<b>CLAHE</b>
0.3880	0.2693
0.5967	0.4589
0.2569	0.2023
0.5698	0.3566
0.4589	0.401
0.359	0.298
0.2963	0.265

Mean square error for various mammogram images:

<b>HISTOGRAM EQUALISATION</b>	<b>CLAHE</b>
0.058	6.0596
0.096	5.9865
0.0986	5.9688
0.1566	12.054
0.1056	9.4579
0.039	6.2579
0.069	7.598

## **CHAPTER 6**

### **CONCLUSION AND FUTURE WORKS**

In this project, the pre processing, segmentation and 3D reconstruction of Mammogram images are discussed. Median filtering proves efficient in noise removal. It is an easy method to denoise the images by using the median values of the matrix. Histogram equalization and CLAHE(Contrast Limited Adaptive Histogram Equalization) is effective for image enhancement. The CLAHE method does not make the contrast of the image to fade while equalizing histogram. The image segmentation gives best result with Adaptive K means algorithm by segmenting the pectoral muscles which belongs to brightest cluster. The tumor is also segmented by using adaptive k-means clustering algorithm. The depth map generation using stereo matching produces accurate values comparing to the image classification method. Since the depth map produces the segmented tumor classified by using surface plot of the disparity between them. The 3D reconstruction of tumor present in the mammogram images can be accomplished by radon transform. Radon transform analyse for each step of angles to match the pixel correspondences by projection.

#### **FUTURE WORKS**

The future works include the following step:

- classification of features from the reconstructed image

## REFERENCES

- [1] Sara Deghani and MashallahAbbasiDezfooli "A Method For Improve Pre processing Images" Mammography International Journal of Information and Education Technology, Vol. 1, No. 1, April 2011.
- [2] Ernest L. Hall, Richard P. Kruger, Samuel J. Dwyer, Iii, David L. Hall, Robert W. McLaren and GwilymS.Lodwick " A Survey of Pre processing and Feature Extraction Techniques for Radiographic Images" IEEE Transactions On Computers, Vol. C-20, No. 9, September 1971.
- [3] R. Beulah Jeyavathana<sup>1</sup>, Dr.R.Balasubramanian<sup>2</sup>, A. AnbarasaPandian "A Survey: Analysis on Pre-processing and Segmentation Techniques for Medical Images" International Journal of Research and Scientific Innovation (IJRSI) | Volume III, Issue VI, June 2016.
- [4] D.NarainPonraj, M.Evangelin Jenifer, P. Poongodi, J.SamuelManoharan "A Survey on the Pre processing Techniques of Mammogram for the Detection of Breast Cancer VOL. 2, NO. 12, December 2011 Journal of Emerging Trends in Computing and Information Sciences.
- [5] Rangaraj M. RangayyanUniversity of Calgary, Calgary, Alberta, Canada "Biomedical Image Analysis".
- [6] Farag H. Alhsnony "A New Technique for Pectoral Muscle Detection" International Journal of Modeling and Optimization, Vol. 3, No. 2, April 2013.
- [7] Mariam Biltawi<sup>1</sup>, Nijad Al-Najdawi<sup>2</sup>, Sara Tedmori<sup>3</sup> "Mammogram Enhancement And Segmentation Methods:Classification, Analysis, And Evaluation" The 13th International Arab conference on Information Technology ACIT2012 Dec.10-13.
- [8] Wiro J. Niessen Max A. Viergever "Medical Image Computing and Computer-Assisted Intervention" – MICCAI 2014th International ConferenceUtrecht, The Netherlands, October 14-17, 2001 Proceedings.
- [9] Nicholas AyacheHervéDelingettePolinaGollandKensaku Mori "Medical Image Computing and Computer-AssistedIntervention" –MICCAI 2012-15th International Conference Nice, France, October 1-5, 2012 Proceedings, Part I.
- [10] InêsDomingues, Jaime S. Cardoso, Member, Igor Amaral, Inês Moreira, Pedro Passarinho, João Santa Comba, Ricardo Correia, Maria J. Cardoso "Pectoral muscle detection in mammograms based on the shortest path with endpoints learnt by SVMs"32nd Annual

International Conference of the IEEE EMBS Buenos Aires, Argentina, August 31 - September 4, 2010.

[11] Sreedevi S, Elizabeth Sherly "A Novel Approach for Removal of pectoral muscles in Digital Mammogram" International Conference on Information and Communication Technologies (ICICT 2014).

[12] R.Poongothai, I.LaurenceAroquiaraj, D.Kalaivani "A Novel Pectoral Removal Approach in Digital Mammogram Segmentation and USRR Feature Selection" International Journal of Engineering Research and Applications.

[13] Muhammad WaseemKhan "A Survey: Image Segmentation Techniques" International Journal of Future Computer and Communication, Vol. 3, No. 2, April 2014

[14] IndraKantaMaitra, Sanjay Nag, Samir K Bandyopadhyay "Accurate Breast Contour Detection Algorithms in Digital Mammogram" International Journal of Computer Applications (0975 – 8887) Volume 25– No.5, July 2011.

[15] SuhasSapate and Sanjay Talbar "An Overview of Pectoral Muscle Extraction Algorithms Applied to Digital Mammograms".

[16] Sami S. Brandt, GopalKaremore, NicoKarssemeijer, and Mads Nielsen, "Anatomically Oriented Breast Coordinate System for Mammogram Analysis".

[17] R. J. Ferrari, R. M. Rangayyan, , J. E. L. Desautels, R. A. Borges, and A. F. Frère "Automatic Identification of the Pectoral Muscle in Mammograms" IEEE Transactions On Medical Imaging, Vol. 23, No. 2, February 2004.

[18] M. Molinara, C. Marrocco, F. Tortorella" Automatic Segmentation of the Pectoral Muscle in Mediolateral Oblique Mammograms".

[19] TodorGeorgiev ,SalilTambe, Andrew Lumsdaine, Jennifer Gille, Ashok Veeraraghavan "The Radon Image As Plenoptic Function".

[20] Hitiksha Shah "Automatic Suppression of Pectoral Muscle in Digital Mammogram using Triangular Mask" 1st International Conference on Advent Trends in Engineering, Science and Technology "ICATEST 2015", 08 March 2015.

[21] David Raba, Arnau Oliver, Joan Mart, Marta Peracaula, and Joan Espunya "Breast Segmentation with Pectoral Muscle Suppression on Digital Mammograms".

- [22] R. Ramani, Dr. S. Suthanthiravanitha, S. Valarmathy "A Survey Of Current Image Segmentation Techniques For Detection Of Breast Cancer International Journal of Engineering Research and Applications (IJERA) Vol. 2, Issue 5, September- October 2012.
- [23] A. KajaMohideen, PSG College of Technology, Coimbatore, India K. Thangavel "Removal of Pectoral Muscle Region in Digital Mammograms using Binary Thresholding" International Journal of Computer Vision and Image Processing, 2(3), 21-29, July-September 2012 21.
- [24] Nirmal Joseph, Shiji T P, Rekha Lakshmanan, Vinu Thomas "Detection And Approximation Of Pectoral Muscle Using Median Filtering And Gray Level Thresholding".
- [25] Nico Karssemeijer, Martin Thijssen, Jan Hendriks and Leon van Erning "Digital Mammography" Nijmegen, 1998
- [26] Alan C. Bovik, Supervisor Mia K. Markey, Supervisor John A. Pearce John E. Gilbert Gary J. Whitman "Evidence-based Detection of Spiculated Lesions on Mammography".
- [27] Jaime S. Cardoso, Inês Domingues, Igor Amaral, Inês Moreira, Pedro Passarinho, João Santa Comba, Ricardo Correia, Maria J. Cardoso "Pectoral muscle detection in mammograms based on polar coordinates and the shortest path".
- [28] Inês Domingues, Jaime S. Cardoso, Igor Amaral "Pectoral muscle detection in mammograms based on the shortest path with endpoints learnt by SVMs".
- [29] Li Liu & Qian Liu & Wei Lu "Pectoral Muscle Detection in Mammograms Using Local Statistical Features"
- [30] Patrik Kamencay, Martin Breznan, Roman Jarina, Peter Lukac, Martina Zachariasova, "Improved Depth Map Estimation from Stereo Images Based on Hybrid Method", Dept. of Telecommunications and Multimedia, University of Zilina, Univerzitna 8215/1, 010 26 Zilina, Slovakia.
- [31] Wenqi Zhu, "3D Reconstruction From Multiple Views Based on Scale-Invariant Feature Transform".
- [32] M. Nießner and A. Dai and M. Fisher, "Combining Inertial Navigation and ICP for Real-time 3D Surface Reconstruction", Short Paper.
- [33] Chuchart Pintavirooj and Manas Sangworasil, "3D-shape reconstruction based on radon transform with application in volume measurement", Research Center for Communications and Information Technology.

- [34] Sanjiv K. Bhatia, "Adaptive K-Means Clustering" Department of Mathematics & Computer Science University of Missouri – St. Louis.
- [35] Amir Averbuch, Ilya Sedelnikov, and Yoel Shkolnisky, "CT Reconstruction From Parallel And Fan-Beam Bprojections By A 2-D Discrete Radon Transform ", IEEE transactions on image processing, vol. 21, no. 2, february 2012.
- [36] Ljubis̃ A Stankovic, Thayananthan Thayaparan, Vesna Popovic' Bugarin, "Inverse Radon Transform–Based Micro-Doppler Analysis From A Reduced Set Of Observations", manuscript received january 5, 2014; revised august 5, 2014, october 30, 2014; released for publication november 21, 2014.
- [37] William h. Press, "Discrete Radon Transform Has An Exact, Fast Inverse And Generalizes To Operations Other Than Sums Along Lines", losalamos national laboratory, los alamos, nm 87545.
- [38] Sigurdur Helgason, "Radon Transform Second Edition".
- [39] Yu Jeffrey Gu & Mauricio Sacchi, "Radon Transform Methods And Their Applications In Mapping Mantle Reflectivity Structure" springerscience+business media b.v. 2009.
- [40] Stanley r. Deans, "Radon And Abel Transforms." The transforms and applications handbook: second edition.
- [41] Kartik Saxena, Pankaj Gautam, "Iterative Closest Point Algorithm 3d Computer Vision - Project Report".
- [42] Rong Zhu, Yong Wang, "Application Of Improved Median Filter On Image Processing", journal of computers, vol. 7, no. 4, april 2012.
- [43] Peng Lei, "Adaptive Median Filtering Seminar Report".
- [44] Manjinder Kaur, Navjot Kaur, Harkamaldeep Singh, "Adaptive K-Means Clustering Techniques For Data Clustering", international journal of innovative research in science, engineering and technology.
- [45] P. Kamencay, m. Breznan, r. Jarina, p. Lukac, m. Zachariasova, "Improved Depth Map Estimation From Stereo Images Based On Hybrid Method" dept. of telecommunications and multimedia, university of zilina, univerzita 8215/1, 010 26 zilina, slovakia.
- [46] Jochen Schmidt, Heinrich Niemann, "Dense Disparity Maps In Real-Time With An Application To Augmented Reality"

## **LIST OF PUBLICATION**

- Presented a paper titled “Survey Of Mammogram Pre-Processing-A Review”at International Conference On Science, Technology, Engineering And Management (ICSTEM’17) at KalaingarKarunanidhi Institute Of Technology.

# KIT - Kalaignarkarunanidhi Institute of Technology



(Accredited with 'A' Grade by NAAC)  
(Approved by AICTE, New Delhi & Affiliated to Anna University, Chennai)  
KIT Global Institute for Advanced Studies & Research  
Coimbatore-641 402, Tamilnadu, India.



ISO 9001:2008  
www.tuv.com  
ID 9100061910

## Certificate of Appreciation

This is to certify that *Dr./Mr./Ms./Prof* ... **NANCY PRIYA** ... & .....  
of **KUMARAGURU COLLEGE OF TECHNOLOGY** ..... has presented  
a paper titled **SURVEY OF MAMMOGRAM PRE-PROCESSING -** .....  
**A REVIEW** ..... in  
ICMR sponsored **IEEE International Conference on Science, Technology,  
Engineering and Management (ICSTEM'17)** held on 3<sup>rd</sup> and 4<sup>th</sup>  
March, 2017 at **KIT - Kalaignarkarunanidhi Institute of Technology, Coimbatore,  
Tamilnadu, India.**

  
**Dr. R. Sukumar**  
Organizing Chair

  
**Dr. P. Anbalagan**  
Director

  
**Dr. N. Mohan Das Gandhi**  
Principal

*In Association with*

